Quantification of Brain Functional Connectivity Deviations in Individuals: A Scoping Review of Functional MRI Studies

Artur Toloknieiev*[1], Dmytro Voitsekhivskyi[1,2], Hlib Kholodkov[1,3], Roman Lvovich[1,4], Petro Matiushko[5], Daria Rekretiuk[3], Andrii Dikhtiar[3], Antonii Viter[3], Volodymyr Pokras[3], Stephan Wunderlich[1], and Sophia Stoecklein†[1]

[1]Department of Radiology, University Hospital, LMU Munich, Munich, Germany

[2]Munich School of Management, LMU Munich, Munich, Germany

[3]School of Computation, Information and Technology, Technical University of Munich, Munich, Germany

[4]Faculty of Electrical Engineering and Information Technology, Technical University of Munich, Munich, Germany

[5]Faculty of Mathematics, Computer Science and Statistics, LMU Munich, Munich, Germany

December 2024

Abstract

Functional connectivity magnetic resonance imaging (fcMRI) is a well-established technique for studying brain networks in both healthy and diseased individuals. However, no fcMRI-based biomarker has yet achieved clinical relevance. To establish better understanding of the state of the art in quantifying abnormal connectivity in comparison to a reference distribution, for potential use in individual patients, we have conducted a scoping review over 5672 entries from the last 10 years. We have located five publications proposing methods of abnormal connectivity quantification, reported these methods and formalized them. We also illustrated the emerging trends and technical innovations in fcMRI research that may facilitate development of individualized fcMRI-based abnormal connectivity metrics.

1 Introduction

Functional connectivity magnetic resonance imaging (fcMRI), first used for connectivity analysis in humans by Biswal et al. [1] and based on the blood oxygen level dependent (BOLD) signal [2, 3, 4], is widely regarded as a valuable imaging method for the inquiry into connectivity in human [5, 6] and non-human [7] brain research alike. With the scientific community increasingly reconceptualizing neurodegenerative [8, 9], psychiatric [10] and neuro-oncological [11, 12, 13] disorders as "network disorders", fcMRI-based biomarkers that quantify abnormal connectivity in relation to the distribution in a healthy reference sample may pave a way for a connectivity metrics suited for validation and application in clinical diagnostics.

To date, no fcMRI biomarker has achieved clinical relevance. This can be

*Corresponding author: tolokniеiev.artur@campus.lmu.de
†Corresponding author: sophia.stoecklein@med.uni-muenchen.de

linked to two major challenges: (1) limited interpretability of the acquired signal in consequence of intra-subject variability and device- and procedure-related confounds [14, 15, 16] and (2) a lack of well-established and readily accessible reference values for functional connectivity in individuals despite available datasets (e.g. Human Connectome Project [52] and 1000connectomes [17]). Alleviating these issues through systematic use of reference samples and normative modeling may permit consistent data interpretation and pave the way for an fcMRI biomarker accessible enough for potential incorporation into diagnostic practice.

In light of the potential benefits of establishing such a normative model for fcMRI, and considering the successful biomarker normalization attempts in other brain imaging modalities [18, 19, 20], two assertions can be made.

Firstly, there exists an apparent unmet medical need for validated and clinically implemented fcMRI-based abnormality metrics that satisfy the criteria of relationality and countability. Herein, a relational metric may be defined as a metric that relies on a control cohort sufficiently representative of the target individual, allowing to establish a normative model of connectivity that compares a given individual to a distribution of controls and quantifies the discrepancy, while a countable metric may be defined as an interval or rational metric that can be used as grounds for grading or comparison.

Secondly, there is minimal study coverage pertaining to the introduction and validation of such metrics, which limits current insight into individualized abnormality detection in functional connectivity.

An initial step toward addressing the question of normative modelling in fcMRI consists in a scoping review of fcMRI-based metrics of connectivity abnormality, the results of which we present here. Within the scope of this paper, we review and analyze the fcMRI abnormality metrics yielded by our search, explore the degree of their refinement, and determine their readiness for clinical

validation. Moreover, we discuss the need of moving beyond group comparison and towards quantitative fcMRI anomaly metrics for application in individual patients. We also elucidate emerging trends and technical innovations in fcMRI research that may facilitate development of relational fcMRI-based abnormality metrics.

2 Methods

2.1 Overall Protocol

We have conducted our review in adherence to the general framework of scoping reviews proposed by Arksey and O'Malley [21] and refined by Levac et al. [22]. We reported our results in compliance with the Preferred Reporting Items for Systematic reviews and Meta-Analyses (PRISMA) extension for scoping reviews (PRISMA-ScR) [23]. The PRISMA-ScR compliance checklist can be accessed in the Supplementary Materials.

2.2 Review Objectives

Within the scope of this review, we intended to determine (1) whether there exist metrics to quantify the deviation of functional connectivity in an individual patient from a reference population, (2) whether they are validated to guarantee sufficient technology readiness and clinical utility and (3) whether they satisfy the criteria of relationality and countability outlined in the introduction.

In pursuit of this objective, we have reviewed the state-of-the-art (SOTA) in fcMRI connectivity abnormality detection, analyzed the results, formalized them, and reported our findings.

2.3 Information Sources, Search Strategy, Data Acquisition and Handling

We have leveraged the Google Scholar database for our seearch. We set the query year range at the years 2014-2024 and employed Publish or Perish 8.10.4612.8838 [24] to automate our query. We searched in 1-year batches to yield the most entries and circumvent the internal limit of 1000 entries per query. We input the following search request: "fcMRI connectivity connectome abnormality detection anomaly map deviation individual reference metric."

All data was aggregated using pandas 2.1.1 [25] and NumPy 1.23.5 [26], exported as comma-separated values, and uploaded for subsequent group review on a secure team space in Notion [27]. Using Notion's integrated tools and functions, we removed damaged or empty entries. The remaining entries were subjected to screening and eligibility assessment (see below).

2.4 Study Screening and Selection

We employed a 2-phase screening and eligibility selection strategy. During the screening phase, we excluded sources that (1) did not report research based on fMRI or did not use BOLD signal, (2) reported experiments on participants under 18 years of age, (3) did not have a healthy reference cohort against which the patients would be gauged, (4) were reviews, (5) were preprints, (6) were book chapters, (7) did not report research on resting-state fcMRI, (8) were not accessible for full text, (9) reported research on data acquired with a field strength under 3.0 T, (10) were theses or dissertations, (11) were meta-analyses, (12) reported research conducted on non-human data, (13) were citation records, (14) were abstract almanacs or miscellaneous publications, (15) were conference papers, (16) were study protocols or (17) were not in English.

Eligibility assessment phase consisted in elimination of articles that did not

report metrics that satisfy the criteria of relationality and countability outlined in the introduction. Eligibility assessment relied on an in-depth inspection of the "Methods" section and a deeper examination of other paper sections in cases where it was necessary. Edge cases were resolved by reviewer consensus.

2.5 Study Analysis

The sources which passed screening and selection were fully studied. Subsequently, we extracted the metric computation methods reported by the respective authors, described them, and formalized them. To explore the degree of their refinement, state of validation, and level of applicability in a clinical setting, we chose to follow the citations of the articles in question (for better narration consistency and text legibility, these searches will be reported within the results section). Subsequently, we integrated these findings to yield our statements. We additionally assigned to every metric a Technology Readiness Level (TRL) as specified by ISO 16290:2013 [28] in the edition of EU Commission Decision C(2017)7124 [29], elucidated for fcMRI-based abnormality detection applications as per Table 1.

3 Results

3.1 Query Results

Our query cumulatively returned 5696 entries, 5672 of them valid (non-empty, not damaged or fragmentary) entries. After screening, 4964 sources were excluded (Fig. 1), while 708 sources were deemed eligible for selection. Only 5 passed selection and were subjected to a full-depth analysis. A PRISMA flow diagram is available in Fig. 2.

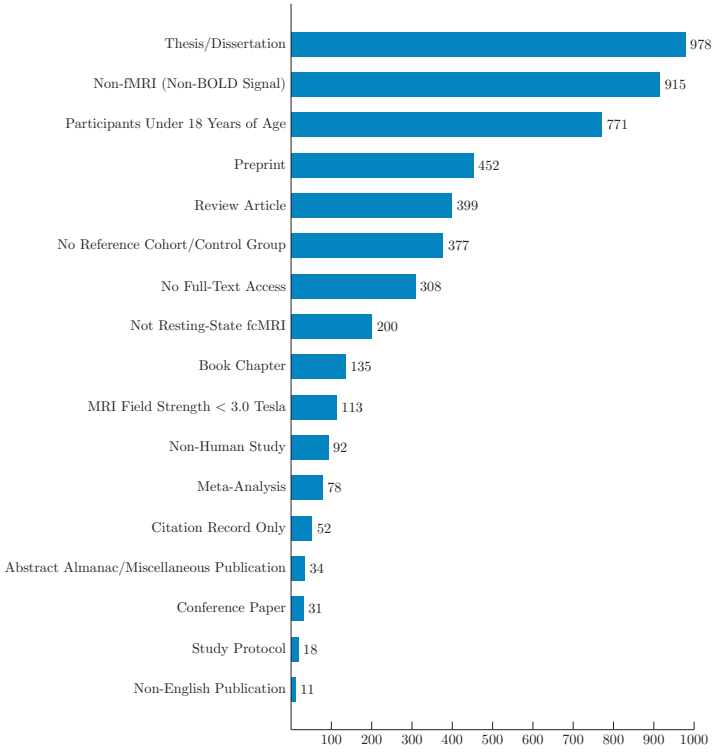

Figure 1: Entries eliminated during Screening phase. In total, we have excluded 4964 entries, of them entries on 978 theses and dissertations, 915 non-fMRI studies, 771 studies on patients under 18 years of age, 452 preprints, 399 reviews, 377 studies without a healthy reference cohort, 308 articles without accessible full-text, 200 non-resting-state fMRI studies, 135 book chapters, 113 studies conducted on data acquired with a field strength under 3.0 Tesla, 92 studies conducted on non-human data, 78 meta-analyses, 52 citation records, 34 abstract almanacs or other publications, 31 conference papers, 18 protocol papers and 11 publications in a language other than English.

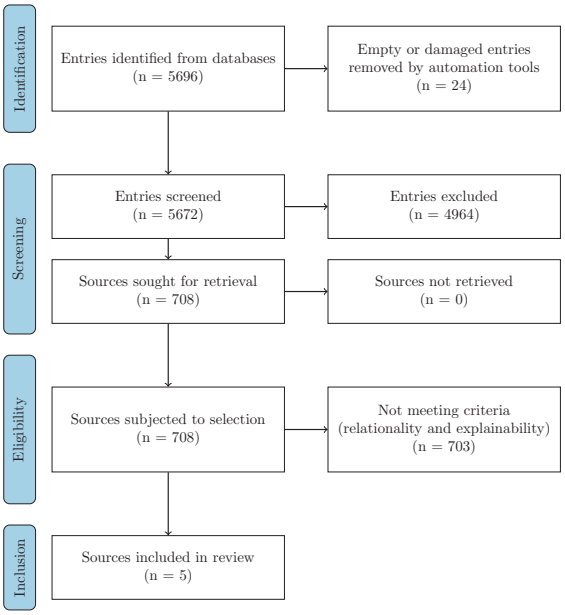

Figure 2: PRISMA flow diagram of review process. In the screening phase we have eliminated 4964 entries of sources (see Section 2.4 and Fig. 1), retrieved 708 sources for review eligibility assessment and applied to them the criteria of relationality and countability outlined previously. Notably, only five sources could be deemed eligible for inclusion into the review.

Table 1: Technology Readiness Levels (TRL) for fcMRI-based abnormality detection

TRL	**Description**	**Elucidation for fcMRI domain**
TRL 1	Basic Principles Observed	Study of BOLD signals and derived functional connectivity metrics at the region of interest (ROI) level; understanding hemodynamic responses in individual ROIs
TRL 2	Technology Concept Formulated	Conceptualizing ROI-wise detection methods; formulating hypotheses on ROI abnormalities
TRL 3	Proof-of-Concept Demonstrated	Simulations with synthetic data or real data with niche cases; initial testing of algorithms in exploratory contexts
TRL 4	Component Validation in Lab Environment	Testing on controlled datasets; refining ROI-wise analysis techniques
TRL 5	Component Validation in Relevant Environment	Application to small-scale real-world human data; adjusting for real-world variability; limited longitudinal studies
TRL 6	Prototype Demonstration in Relevant Environment	Pilot studies with clinical data; collaborating with clinicians for feedback; extensive longitudinal studies
TRL 7	Prototype Demonstration in Operational Environment	Deployment in clinical settings; integration with existing imaging systems; experimental clinical decision support
TRL 8	System Qualified Through Test and Demonstration	Conducting clinical trials; initiating regulatory compliance processes; system/metric validated in clinical contexts for decision support
TRL 9	Actual System Proven in Operational Environment	Widespread clinical adoption; ongoing monitoring and support; ready for long-term integration into clinical guideline

3.2 State of the Art and its Aspects

3.2.1 The Nenning Index

Nenning et al. [30] introduced a voxel-level connectivity abnormality metric in their 2020 glioblastoma paper. Briefly, it is computed as follows: (1) voxel-wise connectivity matrices for both patients and controls (80 control subjects) are built using z-scored Pearson correlations; (2) element-wise average of control population connectivity matrices is computed to yield a group average "normal" connectivity matrix; (3) a vector of voxel-wise differences is computed between the patients and group average as row-wise cosine similarity; (4) for every voxel in controls' connectivity matrices and the group average matrix, cosine similarities are computed to yield voxel-wise distribution; from that distribution, the median and mean absolute deviation (MAD) are computed (the "voxel mean" and "voxel MAD" respectively); (5) for every patient and for every patient voxel's cosine similarity, an abnormality score is computed as the difference of cosine similarity and voxel mean, subsequently divided by the voxel MAD.

Analytically, this can be summarized as follows:

$$A_v^{(p)} = \frac{\dfrac{\mathbf{C}_{v,*}^{(p)} \cdot \overline{\mathbf{C}}_{v,*}}{\left|\mathbf{C}_{v,*}^{(p)}\right| \left|\overline{\mathbf{C}}_{v,*}\right|} - \text{median}\left(\left\{ \dfrac{\mathbf{C}_{v,*}^{(c_i)} \cdot \overline{\mathbf{C}}_{v,*}}{\left|\mathbf{C}_{v,*}^{(c_i)}\right| \left|\overline{\mathbf{C}}_{v,*}\right|} \right\}_{i=1}^{N}\right)}{\text{MAD}\left(\left\{ \dfrac{\mathbf{C}_{v,*}^{(c_i)} \cdot \overline{\mathbf{C}}_{v,*}}{\left|\mathbf{C}_{v,*}^{(c_i)}\right| \left|\overline{\mathbf{C}}_{v,*}\right|} \right\}_{i=1}^{N}\right)} \tag{1}$$

where $C_{v,*}^{(p)}$ is the connectivity vector of voxel v for patient p, $C_{v,*}^{(c_i)}$ is the connectivity vector of voxel v for control subject c_i, with $i = 1, 2, \ldots, N$ and $N = 80$ being the number of control subjects, $\overline{C}_{v,*}$ is the average connectivity vector of voxel v across all control subjects, $\|\cdot\|$ denotes the Euclidean norm of a vector, $\cdot$ represents the dot product between two vectors, median$(\cdot)$ computes the median

of a set of values and MAD(·) computes the median absolute deviation of a set of values.

It is important to mention that Nenning's team focused on reporting abnormality in non-infiltrated regions but pointed out that the inclusion of tumor infiltrated regions did not significantly alter the overall connectivity signature. Additionally, they demonstrate that in glioblastoma, functional proximity to the tumor tends to be reflected stronger than structural proximity in coefficients derived from fcMRI signal, while visual, somatomotor, and limbic networks tend to exhibit anomaly coefficients more evenly informed by both spatial and functional distance alike. Finally, Nenning's team demonstrate precedence of network anomalies before tumor recurrence, highlighting a potential prognostic capacity for abnormality index computation.

PubMed citation check revealed no further studies employing this index in their computations; however, the longitudinal character of the study in focus supports the assignment to this index of a TRL 5 out of 9.

3.2.2 The Dysconnectivity Index

Stoecklein and Liu [31] present another voxel-level connectivity abnormality metric in their publication on gliomas. It is computed as follows: (1) voxel-wise connectivity matrices are built for both patients and controls (1000 control subjects) using Pearson correlations; (2) for every control subject connectivity matrix, every voxel position in the matrix, and every element in the voxel, a distribution of connectivity coefficients is built; (3) the distribution's mean and standard deviation are computed to yield respective elements of the mean and standard deviation vectors; (4) for every patient connectivity matrix, every voxel position in the matrix, and every element in the voxel, a z-score is computed for using the elements of the mean and standard deviation vectors computed before (i.e., for i-th element in the patient's voxel, respective i-th element of the mean

and standard deviation vector is used) to yield a vector of z-scores; (5) a sum of z-scores higher than a specific threshold is computed to yield the voxel-level "abnormality coefficient."

Analytically, for the voxel at the position i this can be summarized as follows:

$$\text{Abnormality Coefficient} = \sum_{j} \mathbb{I}\left(\frac{P^{ij} - \left(\frac{1}{N} \sum_{c=1}^{N} C_c^{ij} \right)}{\sqrt{\frac{1}{N} \sum_{c=1}^{N} \left(C_c^{ij} - \frac{1}{N} \sum_{c=1}^{N} C_c^{ij} \right)^2}} > T \right) \quad (2)$$

where P^{ij} is the connectivity coefficient at voxel position i, j for the patient, C_c^{ij} is the connectivity coefficient at voxel position i, j for control subject c, N is the number of control subjects, T is the specific threshold, and $\mathbb{I}(\cdot)$ is the indicator function, which evaluates to 1 if the condition is true and 0 otherwise.

The authors have conducted computations for the entire brain (without tumor mask exclusion) and demonstrated not only that tumor sites can be captured by their index, but that abnormality can be detected far beyond the lesion itself, even in the contralateral hemisphere, particularly in high grade gliomas. They have also shown that, in glioma, their abnormality index correlates with neurocognitive performance, WHO grade, PET metabolic data, and IDH mutation status. Additionally, the authors hypothesized that abnormal connectivity may not only originate from tumor functional or structural proximity but also indicate sub-clinical tumor cell infiltration and speculated that functional disruption also indicates possible tumor cell infiltration.

PubMed citation check revealed two studies based on this index. In the first publication [32], the authors demonstrated that their abnormality index (in more recent sources referred to as DCI - the "dysconnectivity index") can be employed to assess immune effector cell-associated neurotoxicity syndrome

(ICANS) in patients under CAR-T therapy and hypothesized that it may be used to objectify damage to functional networks in encephalopathies; furthermore, the authors stated that their index may provide an imaging correlate to trace and possibly predict neurotoxic side-effects of oncologic treatment. In the second publication [33], the authors show a direct association between the DCI and the perifocal edema volume in meningiomas, as well as neurocognitive performance (i.e., higher DCI implies larger edema and more degraded cognition).

The sizable body of knowledge amassed in relation to this index, as well as validation for different diseases of the human brain and their sequelae, allows us to assign to this index a TRL of 6 out of 9.

3.2.3 The Doucet Normative Person-Based Similarity Index

In their publication, Doucet et al. [34] report the normative person-based similarity index (nPBSI). Computed from both functional connectivity and cortical morphometry per aspect, their index explicitly seeks to make a patient's condition relative to a set control population (93 control subjects). Doucet's group presents four indices for which clinical, genetic, demographic, and environmental correlates have been described - normative cortical thickness PBSI (nPBSI-CT), normative subcortical volume PBSI (nPBSI-SV), normative module cohesion PBSI (nPBSI-MC) and normative module integrations (nPBSI-MI).

Within the scope of this review, our attention was focused on the fcMRI-based module cohesion and module integration metrics, computed as follows: (1) the patient's brain is parcellated into default mode, central executive, salience, sensorimotor, and visual networks; (2) within-module connectivity is represented as the average value of a voxel wise z-transformed Pearson correlation coefficient between all of the module's voxel pairs and used to build a patient's module cohesion profile, encoded as a module cohesion feature vector; (3) between-module connectivity is represented as z-transformed Pearson cor-

relation coefficients of the modules' averaged time series and used to build a patient's module integrations profile, encoded as a module integrations feature vector, and finally, (4) the nPBSI-MC or nPBSI-MI are computed as averaged Spearman correlations between the patient and the healthy controls' respective (module cohesion or module integrations) feature vectors.

Analytically, for the patient p this can be summarized as follows:

$$\text{nPBSI-MC} = \frac{1}{|H|} \sum_{h \in H} \rho \left(\left[\frac{1}{K_i} \sum_{(v_p, v_q) \in M_i} z\left(r^{(p)}_{v_p v_q} \right) \right]_{i=1}^{N}, \left[\frac{1}{K_i} \sum_{(v_p, v_q) \in M_i} z\left(r^{(h)}_{v_p v_q} \right) \right]_{i=1}^{N} \right) \tag{3}$$

$$\text{nPBSI-MI} = \frac{1}{|H|} \sum_{h \in H} \rho \left(\left[z\left(r^{(p)}_{M_i M_j} \right) \right]_{i \neq j}, \left[z\left(r^{(h)}_{M_i M_j} \right) \right]_{i \neq j} \right), \tag{4}$$

where N represents the number of brain modules (default mode, central executive, salience, sensorimotor, and visual networks), M_i is the set of voxels in module i, K_i is the number of voxel pairs in module i, $r^{(p)}_{v_p v_q}$ is the Pearson correlation coefficient between voxels v_p and v_q for the patient p, $r^{(h)}_{v_p v_q}$ is the Pearson correlation coefficient between voxels v_p and v_q for a healthy control h, $r^{(p)}_{M_i M_j}$ is the Pearson correlation coefficient between the average time series of modules i and j for the patient p, $r^{(h)}_{M_i M_j}$ is the same for a healthy control h, $z(r) = \frac{1}{2} \ln\left(\frac{1+r}{1-r} \right)$ is the Fisher z-transformation, ρ denotes the Spearman correlation coefficient, H is the set of healthy controls and $|H|$ is the number of healthy controls.

PubMed citation check revealed no studies employing the normative index from this publication in their computations of functional connectivity metrics. The closest possible match [35] relied on computing both the within- and between-network connectivity but did not compute the nPBSI itself. Modest validation for bipolar disorder and lack of nPBSI validation for other disorders justifies the assignment to this metric of a TRL 4 out of 9.

3.2.4 The Network Topography Spatial Similarity Index

Silvestri and Corbetta present a spatial similarity index (SSI) for network topographies derived from independent component analysis (ICA) in their 2022 publication on gliomas [36]. Briefly, it is computed as follows: (1) rs-fcMRI data of the control population (308 individuals) are subjected to a group ICA (G-ICA) to yield group-level template independent component (IC) maps for ten functional networks (specifically, visual, sensorimotor, auditory, cingulo-opercular, dorsal attention, fronto-parietal, default mode, cognitive control, frontal and language networks); (2) the group-level template IC maps are used as spatial constraints for group information-guided ICA (GIG-ICA) of both controls and patients (24 individuals) to produce individual-specific, single-subject level IC maps; (3) for each IC in subject, a cosine similarity is computed between a single-subject IC map and a template IC map thresholded at a value of 1 and is yielded as the network topography spatial similarity index.

Analytically, this can be expressed as follows:

$$SSI_{IC} = \frac{\left(\text{GIG-ICA}\left(D_s; \{T_k\}_{k=1}^{10}\right)_j\right) \cdot \left(\text{Threshold}_1(T_j)\right)}{\left\|\text{GIG-ICA}\left(D_s; \{T_k\}_{k=1}^{10}\right)_j\right\| \cdot \left\|\text{Threshold}_1(T_j)\right\|} \tag{5}$$

where SSI_{IC} is the spatial similarity index for a given independent component, $D = \{D_i\}_{i=1}^{308}$ represents the rs-fMRI data of the control population, $T = \text{G-ICA}(D) = \{T_j\}_{j=1}^{10}$ are the group-level template IC maps for the ten functional networks obtained from group ICA, D_s is the rs-fMRI data of subject s, $\text{GIG-ICA}(D_s; \{T_k\}_{k=1}^{10})_j$ produces the single-subject IC map $S_{s,j}$ for subject s and component j using the group-level templates as spatial constraints, $\text{Threshold}_1(T_j)$ denotes the template IC map T_j thresholded at a value of 1, the numerator $(\cdot)$ represents the dot product between the two vectors and the denominator $(\|\cdot\|)$ represents the Euclidean norm (magnitude) of the vectors.

The team around Silvestri and Corbetta reported testing structural and functional proximity of their index to the tumor sites, describing partial overlap of index abnormalities and glioma-infiltrated areas and highlighting index abnormalities in non-infiltrated areas. They also analyzed changes in network topography scores and neuropsychological performance and were able to capture a statistically relevant relationship between the SSI and the attention domain. PubMed citation check revealed no studies employing this normative index in their computations of functional connectivity metrics. Modest validation for gliomas and lack of validation for other disorders justifies the assignment to this metric of a TRL 4 out of 9.

3.2.5 The Morgan Network Topology Method

Morgan et al. present various metrics and indices in their publication on the role of anterior hippocampus in mesial temporal lobe epilepsy (mTLE) [37]. Their computations rely on multi-modal data and operate within four topologies: the streamline length (T_{LEN}), structural connectivity (T_{SC}), functional connectivity (T_{FC}) and resting-state network topology (T_{RSN}). Within the scope of our review, we will focus on the functional connectivity topology and its respective distance index, as no similar index has been reported for the resting-state network topology.

Briefly, it is computed as follows: (1) functional connectivity maps are built for controls (70 individuals) and patients (40 individuals, of them 29 with right mTLE and 11 with left mTLE) from z-transformed functional connectivity matrices through age regression and subsequent averaging of signal over 109 anatomical ROIs; (2) a topology is built from the functional connectivity maps by selecting 55 ROIs of a single hemisphere for patients and controls; (3) a seed vector is used to slice anterior hippocampal connectivity from the topology into a connectivity vector for both patients and controls; (4) the connectivity vec-

tor is stratified along connectivity intensity into "bins" to yield their respective connectivity vectors of k elements for both patients and controls; (5) for patient and bin, the Mahalanobis distance between the patient's bin connectivity vector and the mean of controls' bin connectivity vectors is computed and yielded as connectivity deviation metric.

Analytically, this can be summarized as follows:

$$MD_{i,b} = \sqrt{(\phi_{i,b} - \mu_b)^\top \Sigma_b^{-1} (\phi_{i,b} - \mu_b)} \tag{6}$$

with patient's connectivity vector in bin, controls' mean vector in bin and controls' covariance matrix in bin as, respectively,

$$\phi_{i,b} = B_b\left(RS(M_i)\right) \tag{7}$$

$$\mu_b = \frac{1}{N_c} \sum_{j=1}^{N_c} B_b\left(RS(M_j)\right) \tag{8}$$

and

$$\Sigma_b = \frac{1}{N_c - 1} \sum_{j=1}^{N_c} \left(B_b\left(RS(M_j)\right) - \mu_b\right) \left(B_b\left(RS(M_j)\right) - \mu_b\right)^\top \tag{9}$$

where M_i is a functional connectivity matrix (size 109×109) for individual i, $S(M_i)$ denotes a selection operator extracting a 55×55 hemisphere-specific submatrix from M_i, R is a seed vector (size 1×55) with 1 at the anterior hippocampus position and 0 elsewhere, $B_b(\cdot)$ symbolizes the binning function that selects elements belonging to bin b based on connectivity intensity, $N_c = 70$ is the number of control individuals, μ_b is the mean vector of controls' connectivity vectors in bin b and Σ_b is the covariance matrix of controls' connectivity vectors in bin b.

PubMed citation check revealed two studies which reported intriguing use of the logic behind this computational approach. The first publication of interest

by Morgan et al. [38] reports use of similar connectivity profiling techniques and the Mahalanobis distance for outcome prediction in mTLE patients by means of distance computation between a patient's connectivity profile and a normative population of individuals who achieved seizure-free status after mesial temporal lobe surgery. Notably, the team around Morgan reported sensitivity of 100% and specificity of 90% for their prediction approach.

The second publication by Guerrero-Gonzalez et al. [39] does not pertain to functional MRI, but describes use of the comparable logic of normative modeling and Mahalanobis distance computing to quantify abnormality in tractography of traumatic brain injury patients.

The epilepsy-specific focus of Morgan's distance-based approach limits the scope of potential use of this metric; however, success of similar computational approaches in other modalities and remarkable performance of the Mahalanobis distance-based index in the surgical outcome prediction task support the assignment to this metric of a TRL 5 out of 9.

4 Discussion

4.1 Group Comparison Currently Prevails in Studies of Abnormal Connectivity

In this scoping review, we have been able to show that, despite the strong knowledge base to support the concept of neurodegenerative [8, 9], psychiatric [10] and neuro-oncological [11, 12, 13] as "network disorders", a metric capable of evaluating and quantifying large-scale functional brain network disruptions in individual patients is yet to be developed, validated and made accessible enough for potential incorporation into diagnostic practice.

We also demonstrated that, despite the significant benefits of relational met-

rics as integral elements of normative modeling [40], we could only retrieve five such metrics of functional connectivity deviation that have been proposed within the last ten years. Of note, in many studies that we evaluated for this review, the findings and the hypotheses that lead to these findings were built around the aspiration to illustrate binary differences between patients and healthy controls, which resulted in reports of metrics being increased or decreased in patients without a clearly specified relation between the increment of metric and increment of pathological state. The development of patient-centric fcMRI markers requires moving beyond group comparison and toward relational metrics based on normative populations that span variability in demographic and procedural factors.

4.2 Artificial Intelligence and Big Data Emerge as Methods in fcMRI Research

The advent of big data and artificial intelligence-based methods in fcMRI research may boost the development of relational connectivity metrics by enhancing the current computational approaches and data accessibility.

The drastic progress in computing technology [41] has made possible the widespread use of industrial-grade hardware acceleration of previously strictly linear computing through parallel computing with the help of much more readily accessible graphical processing units (GPUs) [42, 43]. Improved hardware-software synergy now permits optimization of both speed and efficiency of data engineering and machine learning, allowing for faster simultaneous read-/write operations and deeper insight into highly complex multidimensional data. This is well-manifested by the packages for accelerated Python computing (e.g. CuPy[44] or Dask [45]), optimized tensor storage solutions (e.g. Zarr [46] or Xarray [47]), new Neuroimaging Informatics Technology Initiative (NifTI) im-

age manipulation modules (e.g. Xibabel [48]) or the advancements in the field of machine learning (ML) frameworks [49, 50, 51].

Simultaneously, high-quality data can be accessed freely by virtue of recognized cohorts (e.g. Human Connectome Project, Alzheimer's Disease Neuroimaging Initiative or Brain Genomics Superstruct Project [52, 53, 54]) and open-access data repositories (e.g. OpenNeuro [55]), which permits compilation of harmonized, statistically powerful reference datasets, capturing variability across demographics and technical parameters. The utility of accounting for these factors is well-substantiated by evidence of variables such as age [56, 57, 58], sex [59, 60] and scan parameters [61, 62] having significant influence on fcMRI metrics. Therefore, creation of large-scale reference datasets augmented by technical and demographic parameters may help pave the way for normative modelling in fcMRI.

Moreover, the current rise of deep learning models for operations on fcMRI data can help streamline previously time-consuming elements of data preprocessing and enrichment, potentially accelerating research on relational fcMRI-based metrics manyfold. This is prominently exemplified by ML breakthroughs in the area of structural image preprocessing with algorithms such as FastSurfer [63], a deep learning pipeline for brain segmentation, cortical surface reconstruction, cortical label mapping and thickness analyses. Similar advancements have also been reported for affine registration with tools such as SynthMorph [64], a model that resolves a tensor-to-tensor mapping problem for an image pair, yielding a compatible spatial transform. Lastly, experimental ML-boosted integrated pipelines for fcMRI image preprocessing (e.g. DeepPrep [65]) have also been proposed.

In summary, the current circumstances create a uniquely favorable setting for more practical progress on relational fcMRI-based metrics of abnormal con-

nectivity.

4.3 Limitations

Our search only comprises sources released before mid-May 2024. Additionally, our search terms might not include all relevant publications. In particular, preprints, theses and dissertations have been excluded as reports that have not undergone a peer review process. Additionally, not all publications could be accessed for full text. Furthermore, due to considerably less generalizable dynamics of neurobiological development in pediatric and adolescent individuals, a decision was made not to consider publications that concerned persons under 18 years of age. Finally, if a publication matched more than one exclusion criterion during screening, its exclusion was attributed to a single most prominently matching criterion in an effort to prevent redundant statistical entries.

5 Summary

Patients suffering from neuro-oncological, psychiatric and neurodegenerative disorders can benefit from individualized detection and quantification of abnormal functional connectivity. However, no fcMRI-derived biomarkers have yet seen widespread adoption in clinical research or practice. Within the scope of this scoping review, we have asserted both the necessity and the current absence of a well-established relational and countable metric for abnormal functional connectivity in individuals. We have subsequently leveraged the Google Scholar database to retrieve sources that matched our search criteria and subjected them to PRISMA-compliant screening and selection to yield items for subsequent in-depth analysis. We have yielded and demonstrated five currently reported methods/metrics for relational, normative quantification of abnormal connectivity and formalized their computation methods. Building upon our

results, we have discussed the need of moving beyond group comparison and toward quantitative fcMRI anomaly metrics for application in individual patients and briefly elucidated the emerging trends and technical innovations in fcMRI research that may facilitate development of relational metrics of functional connectivity.

Acknowledgements

We would like to thank Julia Ruat for her invaluable support in the management of this project.

Funding Information

S.S. received support through the LMU Investment Fund (LMU Excellence AOST: 865105-7). Funding sources had no role in the design, implementation, analysis, interpretation, or reporting of this research.

Conflict of Interest

The authors have no relevant conflict of interest to declare.

Data Availability Statement

Data sharing is not applicable in the context of this publication, as no datasets were generated or analyzed during this scoping review. The tabular reports of the included and excluded articles are available from the corresponding authors upon reasonable request.

Code Availability Statement

No novel code was generated during the current study. Minimal scripting was done to support data aggregation.

Inclusion and Ethics Statement

This scoping review concerns peer-reviewed publications and therefore does not require ethical approval.

Author Contributions

A. T. - Conceptualization, Methodology Selection & Implementation, Data Collection, Entry Screening, Source Eligibility Selection, Source Analysis, Formalization & Integration of Findings, Original Draft Preparation, Visualization, Review and Editing, Project Administration.

D. V. - Data Collection, Entry Screening, Source Eligibility Selection, Source Analysis, Formalization & Integration of Findings, Original Draft Preparation, Visualization, Review and Editing, Project Administration.

H. K. - Data Collection, Entry Screening, Source Eligibility Selection, Source Analysis, Formalization & Integration of Findings, Original Draft Preparation, Visualization, Review and Editing, Project Administration.

R. L. - Entry Screening, Source Eligibility Selection, Source Analysis, Formalization & Integration of Findings.

P. M. - Entry Screening, Source Eligibility Selection.

D. R. - Entry Screening, Source Eligibility Selection.

A. D. - Entry Screening.

A. V. - Entry Screening.

V. P. - Entry Screening.

S. W. - Source Eligibility Selection, Source Analysis.

S. S. - Conceptualization, Source Analysis, Formalization & Integration of Findings, Review and Editing, Supervision, Funding Acquisition, Project Administration, Resources, Oversight and Approvals.

D.V. and H.K. contributed equally to this publication.

D.R. and P.M. contributed equally to this publication.

A.D. and A.V. contributed equally to this publication.

References

[1] Biswal, B., Yetkin, F. Z., Haughton, V. M., & Hyde, J. S. (1995). Functional connectivity in the motor cortex of resting human brain using echo-planar MRI. Magnetic Resonance in Medicine, 34(4), 537–541. https://doi.org/10.1002/mrm.1910340409

[2] Ogawa, S., Lee, T. M., Kay, A. R., & Tank, D. W. (1990). Brain magnetic resonance imaging with contrast dependent on blood oxygenation. Proceedings of the National Academy of Sciences, 87(24), 9868–9872. https://doi.org/10.1073/pnas.87.24.9868

[3] Logothetis, N. K. (2003). The underpinnings of the BOLD Functional Magnetic Resonance Imaging signal. Journal of Neuroscience, 23(10), 3963–3971. https://doi.org/10.1523/jneurosci.23-10-03963.2003

[4] Buxton, R. B., Wong, E. C., & Frank, L. R. (1998). Dynamics of blood flow and oxygenation changes during brain activation: The balloon model. Magnetic Resonance in Medicine, 39(6), 855–864. https://doi.org/10.1002/mrm.1910390602

[5] Buckner, R. L., Krienen, F. M., & Yeo, B. T. T. (2013). Opportunities and limitations of intrinsic functional connectivity MRI. Nature Neuroscience, 16(7), 832–837. https://doi.org/10.1038/nn.3423

[6] Zhang, J., Kucyi, A., Raya, J., Nielsen, A. N., Nomi, J. S., Damoiseaux, J. S., Greene, D. J., Horovitz, S. G., Uddin, L. Q., & Whitfield-Gabrieli, S. (2021). What have we really learned from functional connectivity in clinical populations? NeuroImage, 242, 118466. https://doi.org/10.1016/j.neuroimage.2021.118466

[7] Pagani, M., Gutierrez-Barragan, D., De Guzman, A. E., Xu, T., & Gozzi, A. (2023). Mapping and comparing fMRI connectivity networks across species. Communications Biology, 6(1). https://doi.org/10.1038/s42003-023-05629-w

[8] Franzmeier, N., Dewenter, A., Frontzkowski, L., Dichgans, M., Rubinski, A., Neitzel, J., Smith, R., Strandberg, O., Ossenkoppele, R., Buerger, K., Duering, M., Hansson, O., & Ewers, M. (2020). Patient-centered connectivity-based prediction of tau pathology spread in Alzheimer's disease. Science Advances, 6(48). https://doi.org/10.1126/sciadv.abd1327

[9] Rauchmann, B., Brendel, M., Franzmeier, N., Trappmann, L., Zaganjori, M., Ersoezlue, E., Morenas-Rodriguez, E., Guersel, S., Burow, L., Kurz, C., Haeckert, J., Tatò, M., Utecht, J., Papazov, B., Pogarell, O., Janowitz, D., Buerger, K., Ewers, M., Palleis, C., . . . Perneczky, R. (2022). Microglial activation and connectivity in Alzheimer disease and aging. Annals of Neurology, 92(5), 768–781. https://doi.org/10.1002/ana.26465

[10] Georgiadis, F., Larivière, S., Glahn, D., Hong, L. E., Kochunov, P., Mowry, B., Loughland, C., Pantelis, C., Henskens, F. A., Green, M. J., Cairns, M. J., Michie, P. T., Rasser, P. E., Catts, S., Tooney, P., Scott,

R. J., Schall, U., Carr, V., Quidé, Y., . . . Kirschner, M. (2024). Connectome architecture shapes large-scale cortical alterations in schizophrenia: a worldwide ENIGMA study. Molecular Psychiatry, 29(6), 1869–1881. https://doi.org/10.1038/s41380-024-02442-7

[11] Winkler, F., Venkatesh, H. S., Amit, M., Batchelor, T., Demir, I. E., Deneen, B., Gutmann, D. H., Hervey-Jumper, S., Kuner, T., Mabbott, D., Platten, M., Rolls, A., Sloan, E. K., Wang, T. C., Wick, W., Venkataramani, V., & Monje, M. (2023). Cancer neuroscience: State of the field, emerging directions. Cell, 186(8), 1689–1707. https://doi.org/10.1016/j.cell.2023.02.002

[12] Hausmann, D., Hoffmann, D. C., Venkataramani, V., Jung, E., Horschitz, S., Tetzlaff, S. K., Jabali, A., Hai, L., Kessler, T., Azoŕin, D. D., Weil, S., Kourtesakis, A., Sievers, P., Habel, A., Breckwoldt, M. O., Karreman, M. A., Ratliff, M., Messmer, J. M., Yang, Y., . . . Winkler, F. (2022). Autonomous rhythmic activity in glioma networks drives brain tumour growth. Nature, 613(7942), 179–186. https://doi.org/10.1038/s41586-022-05520-4

[13] Salvalaggio, A., Pini, L., Bertoldo, A., & Corbetta, M. (2024). Glioblastoma and brain connectivity: the need for a paradigm shift. The Lancet Neurology, 23(7), 740–748. https://doi.org/10.1016/s1474-4422(24)00160-1

[14] Rogers, B. P., Morgan, V. L., Newton, A. T., & Gore, J. C. (2007b). Assessing functional connectivity in the human brain by fMRI. Magnetic Resonance Imaging, 25(10), 1347–1357. https://doi.org/10.1016/j.mri.2007.03.007

[15] Duncan, N., & Northoff, G. (2013). Overview of potential procedural and participant- related confounds for neuroimaging of the rest-

ing state. Journal of Psychiatry and Neuroscience, 38(2), 84–96. https://doi.org/10.1503/jpn.120059

[16] Mueller, S., Wang, D., Fox, M. D., Yeo, B. T., Sepulcre, J., Sabuncu, M. R., Shafee, R., Lu, J., & Liu, H. (2013). Individual variability in functional connectivity architecture of the human brain. Neuron, 77(3), 586–595. https://doi.org/10.1016/j.neuron.2012.12.028

[17] Mennes, M., Biswal, B. B., Castellanos, F. X., & Milham, M. P. (2012). Making data sharing work: The FCP/INDI experience. NeuroImage, 82, 683–691. https://doi.org/10.1016/j.neuroimage.2012.10.064

[18] Chamberland, M., Genc, S., Tax, C. M. W., Shastin, D., Koller, K., Raven, E. P., Cunningham, A., Doherty, J., Van Den Bree, M. B. M., Parker, G. D., Hamandi, K., Gray, W. P., & Jones, D. K. (2021). Detecting microstructural deviations in individuals with deep diffusion MRI tractometry. Nature Computational Science, 1(9), 598–606. https://doi.org/10.1038/s43588-021-00126-8

[19] Nugent, S., Croteau, E., Potvin, O., Castellano, C., Dieumegarde, L., Cunnane, S. C., & Duchesne, S. (2020). Selection of the optimal intensity normalization region for FDG-PET studies of normal aging and Alzheimer's disease. Scientific Reports, 10(1). https://doi.org/10.1038/s41598-020-65957-3

[20] López-González, F. J., Silva-Rodríguez, J., Paredes-Pacheco, J., Niñerola-Baizán, A., Efthimiou, N., Martín-Martín, C., Moscoso, A., Ruibal, Á., Roé-Vellvé, N., & Aguiar, P. (2020). Intensity normalization methods in brain FDG-PET quantification. NeuroImage, 222, 117229. https://doi.org/10.1016/j.neuroimage.2020.117229

[21] Arksey, H., & O'Malley, L. (2005). Scoping studies: towards a methodological framework. International Journal of Social Research Methodology, 8(1), 19–32. https://doi.org/10.1080/1364557032000119616

[22] Levac, D., Colquhoun, H., & O'Brien, K. K. (2010). Scoping studies: advancing the methodology. Implementation Science, 5(1). https://doi.org/10.1186/1748-5908-5-69

[23] Tricco, A. C., Lillie, E., Zarin, W., O'Brien, K. K., Colquhoun, H., Levac, D., Moher, D., Peters, M. D., Horsley, T., Weeks, L., Hempel, S., Akl, E. A., Chang, C., McGowan, J., Stewart, L., Hartling, L., Aldcroft, A., Wilson, M. G., Garritty, C., . . . Straus, S. E. (2018). PRISMA Extension for Scoping Reviews (PRISMA-SCR): Checklist and explanation. Annals of Internal Medicine, 169(7), 467–473. https://doi.org/10.7326/m18-0850

[24] Harzing, A.W. (2007) Publish or Perish, available from https://harzing.com/resources/publish-or-perish

[25] McKinney, W. (2010). Data structures for statistical computing in Python. Proceedings of the Python in Science Conferences, 56–61. https://doi.org/10.25080/majora-92bf1922-00a

[26] Harris, C. R., Millman, K. J., Van Der Walt, S. J., Gommers, R., Virtanen, P., Cournapeau, D., Wieser, E., Taylor, J., Berg, S., Smith, N. J., Kern, R., Picus, M., Hoyer, S., Van Kerkwijk, M. H., Brett, M., Haldane, A., Del Río, J. F., Wiebe, M., Peterson, P., . . . Oliphant, T. E. (2020). Array programming with NumPy. Nature, 585(7825), 357–362. https://doi.org/10.1038/s41586-020-2649-2

[27] Your connected workspace for wiki, docs & projects — Notion. (04.12.24). Notion. https://www.notion.so/

[28] ISO 16290:2013. (04.12.24). ISO. https://www.iso.org/standard/56064.html

[29] Research and innovation. (04.12.24). European Commission. `https://ec.europa.eu/research/participants/data/ref/h2020/other/wp/2018-2020/annexes/h2020-wp1820-annex-g-trl_en.pdf`

[30] Nenning, K., Furtner, J., Kiesel, B., Schwartz, E., Roetzer, T., Fortelny, N., Bock, C., Grisold, A., Marko, M., Leutmezer, F., Liu, H., Golland, P., Stoecklein, S., Hainfellner, J. A., Kasprian, G., Prayer, D., Marosi, C., Widhalm, G., Woehrer, A., & Langs, G. (2020). Distributed changes of the functional connectome in patients with glioblastoma. Scientific Reports, 10(1). https://doi.org/10.1038/s41598-020-74726-1

[31] Stoecklein, V. M., Stoecklein, S., Galiè, F., Ren, J., Schmutzer, M., Unterrainer, M., Albert, N. L., Kreth, F., Thon, N., Liebig, T., Ertl-Wagner, B., Tonn, J., & Liu, H. (2020). Resting-state fMRI detects alterations in whole brain connectivity related to tumor biology in glioma patients. Neuro-Oncology, 22(9), 1388–1398. https://doi.org/10.1093/neuonc/noaa044

[32] Stoecklein, S., Wunderlich, S., Papazov, B., Winkelmann, M., Kunz, W. G., Mueller, K., Ernst, K., Stoecklein, V. M., Blumenberg, V., Karschnia, P., Bücklein, V. L., Rejeski, K., Schmidt, C., Von Bergwelt-Baildon, M., Tonn, J., Ricke, J., Liu, H., Remi, J., Subklewe, M., . . . Schoeberl, F. (2023). Functional connectivity MRI provides an imaging correlate for chimeric antigen receptor T-cell-associated neurotoxicity. Neuro-Oncology Advances, 5(1). https://doi.org/10.1093/noajnl/vdad135

[33] Stoecklein, V., Wunderlich, S., Papazov, B., Thon, N., Schmutzer, M., Schinner, R., Zimmermann, H., Liebig, T., Ricke, J., Liu, H., Tonn, J., Schichor, C., & Stoecklein, S. (2023). Perifocal Edema in Patients with

Meningioma is Associated with Impaired Whole-Brain Connectivity as Detected by Resting-State fMRI. American Journal of Neuroradiology, 44(7), 814–819. https://doi.org/10.3174/ajnr.a7915

[34] Doucet, G. E., Glahn, D. C., & Frangou, S. (2020). Person-based similarity in brain structure and functional connectivity in bipolar disorder. Journal of Affective Disorders, 276, 38–44. https://doi.org/10.1016/j.jad.2020.06.041

[35] West, A., Hamlin, N., Frangou, S., Wilson, T. W., & Doucet, G. E. (2021). Person-Based Similarity Index for Cognition and its neural correlates in Late Adulthood: Implications for Cognitive Reserve. Cerebral Cortex, 32(2), 397–407. https://doi.org/10.1093/cercor/bhab215

[36] Silvestri, E., Moretto, M., Facchini, S., Castellaro, M., Anglani, M., Monai, E., D'Avella, D., Della Puppa, A., Cecchin, D., Bertoldo, A., & Corbetta, M. (2022). Widespread cortical functional disconnection in gliomas: an individual network mapping approach. Brain Communications, 4(2). https://doi.org/10.1093/braincomms/fcac082

[37] Morgan, V. L., Johnson, G. W., Cai, L. Y., Landman, B. A., Schilling, K. G., Englot, D. J., Rogers, B. P., & Chang, C. (2021). MRI network progression in mesial temporal lobe epilepsy related to healthy brain architecture. Network Neuroscience, 5(2), 434–450. https://doi.org/10.1162/netn_a_00184

[38] Morgan, V. L., Sainburg, L. E., Johnson, G. W., Janson, A., Levine, K. K., Rogers, B. P., Chang, C., & Englot, D. J. (2022). Presurgical temporal lobe epilepsy connectome fingerprint for seizure outcome prediction. Brain Communications, 4(3). https://doi.org/10.1093/braincomms/fcac128

[39] Guerrero-Gonzalez, J. M., Yeske, B., Kirk, G. R., Bell, M. J., Ferrazzano, P. A., & Alexander, A. L. (2022). Mahalanobis distance

tractometry (MaD-Tract) – a framework for personalized white matter anomaly detection applied to TBI. NeuroImage, 260, 119475. https://doi.org/10.1016/j.neuroimage.2022.119475

[40] Marquand, A. F., Kia, S. M., Zabihi, M., Wolfers, T., Buitelaar, J. K., & Beckmann, C. F. (2019). Conceptualizing mental disorders as deviations from normative functioning. Molecular Psychiatry, 24(10), 1415–1424. https://doi.org/10.1038/s41380-019-0441-1

[41] Coyle, D., & Hampton, L. (2023). 21st century progress in computing. Telecommunications Policy, 48(1), 102649. https://doi.org/10.1016/j.telpol.2023.102649

[42] AMD Technical Information Portal. (04.12.24). https://docs.amd.com/v/u/en-US/wp505-versal-acap

[43] NVIDIA RTX Series Datasheets. (04.12.24). NVIDIA. https://resources.nvidia.com/en-us-briefcase-for-datasheets/

[44] R. Okuta, Y. Unno, D. Nishino, S. Hido, and C. Loomis. CuPy: A NumPy-Compatible Library for NVIDIA GPU Calculations. Proceedings of Workshop on Machine Learning Systems (LearningSys) in The Thirty-first Annual Conference on Neural Information Processing Systems (NIPS), 2017 `http://learningsys.org/nips17/assets/papers/paper_16.pdf`

[45] Dask Development Team (2016). Dask: Library for dynamic task scheduling URL http://dask.pydata.org

[46] Alistair Miles, jakirkham, Joe Hamman, Dimitri Papadopoulos Orfanos, M Bussonnier, Josh Moore, David Stansby, Davis Bennett, Tom Augspurger, James Bourbeau, Andrew Fulton, Sanket Verma, Deepak Cherian, Norman Rzepka, Ryan Abernathey, Gregory Lee, Mads R.

B. Kristensen, Zain Patel, Saransh Chopra, ... Shivank Chaudhary. (2024). zarr-developers/zarr-python: v3.0.0-beta.2 (v3.0.0-beta.2). Zenodo. https://doi.org/10.5281/zenodo.14165945

[47] Hoyer, S., & Hamman, J. (2017). xarray: N-D labeled Arrays and Datasets in Python. Journal of Open Research Software, 5(1), 10. https://doi.org/10.5334/jors.148

[48] Matthew-Brett. (04.12.24). GitHub - matthew-brett/xibabel: Piloting a new image object for neuroimaging based on XArray. GitHub. https://github.com/matthew-brett/xibabel

[49] Jax-Ml. (04.12.24). GitHub - jax-ml/jax: Composable transformations of Python+NumPy programs: differentiate, vectorize, JIT to GPU/TPU, and more. GitHub. http://github.com/jax-ml/jax

[50] Martín Abadi, Ashish Agarwal, Paul Barham, Eugene Brevdo, Zhifeng Chen, Craig Citro, Greg S. Corrado, Andy Davis, Jeffrey Dean, Matthieu Devin, Sanjay Ghemawat, Ian Goodfellow, Andrew Harp, Geoffrey Irving, Michael Isard, Rafal Jozefowicz, Yangqing Jia, Lukasz Kaiser, Manjunath Kudlur, Josh Levenberg, Dan Mané, Mike Schuster, Rajat Monga, Sherry Moore, Derek Murray, Chris Olah, Jonathon Shlens, Benoit Steiner, Ilya Sutskever, Kunal Talwar, Paul Tucker, Vincent Vanhoucke, Vijay Vasudevan, Fernanda Viégas, Oriol Vinyals, Pete Warden, Martin Wattenberg, Martin Wicke, Yuan Yu, and Xiaoqiang Zheng. TensorFlow: Large-scale machine learning on heterogeneous systems, 2015. https://tensorflow.org.

[51] Paszke, A., Gross, S., Massa, F., Lerer, A., Bradbury, J., Chanan, G., Killeen, T., Lin, Z., Gimelshein, N., Antiga, L., Desmaison, A., Köpf, A., Yang, E., DeVito, Z., Raison, M., Tejani, A., Chilamkurthy, S., Steiner, B., Fang, L., . . . Chintala, S. (2019). PyTorch: An Imperative

Style, High-Performance Deep Learning Library. arXiv (Cornell University). https://doi.org/10.48550/arxiv.1912.01703

[52] David C. Van Essen, Stephen M. Smith, Deanna M. Barch, Timothy E.J. Behrens, Essa Yacoub, Kamil Ugurbil, for the WU-Minn HCP Consortium. (2013). The WU-Minn Human Connectome Project: An overview. NeuroImage 80(2013):62-79.

[53] Petersen, R. C., Aisen, P. S., Beckett, L. A., Donohue, M. C., Gamst, A. C., Harvey, D. J., Jack, C. R., Jagust, W. J., Shaw, L. M., Toga, A. W., Trojanowski, J. Q., & Weiner, M. W. (2009). Alzheimer's Disease Neuroimaging Initiative (ADNI). Neurology, 74(3), 201–209. https://doi.org/10.1212/wnl.0b013e3181cb3e25

[54] Holmes, A. J., Hollinshead, M. O., O'Keefe, T. M., Petrov, V. I., Fariello, G. R., Wald, L. L., Fischl, B., Rosen, B. R., Mair, R. W., Roffman, J. L., Smoller, J. W., & Buckner, R. L. (2015). Brain Genomics Superstruct Project initial data release with structural, functional, and behavioral measures. Scientific Data, 2(1). https://doi.org/10.1038/sdata.2015.31

[55] OpenNeuro. (04.12.24). https://openneuro.org/

[56] Farras-Permanyer, L., Mancho-Fora, N., Montalà-Flaquer, M., Bartrés-Faz, D., Vaqué-Alcázar, L., Peró-Cebollero, M., & Guàrdia-Olmos, J. (2019). Age-related changes in resting-state functional connectivity in older adults. Neural Regeneration Research, 14(9), 1544. https://doi.org/10.4103/1673-5374.255976

[57] Geerligs, L., Renken, R. J., Saliasi, E., Maurits, N. M., & Lorist, M. M. (2014). A Brain-Wide study of Age-Related changes in functional connectivity. Cerebral Cortex, 25(7), 1987–1999. https://doi.org/10.1093/cercor/bhu012

[58] Andrews-Hanna, J. R., Snyder, A. Z., Vincent, J. L., Lustig, C., Head, D., Raichle, M. E., & Buckner, R. L. (2007). Disruption of Large-Scale brain systems in advanced aging. Neuron, 56(5), 924–935. https://doi.org/10.1016/j.neuron.2007.10.038

[59] David, S. P., Naudet, F., Laude, J., Radua, J., Fusar-Poli, P., Chu, I., Stefanick, M. L., & Ioannidis, J. P. A. (2018). Potential reporting bias in neuroimaging studies of sex differences. Scientific Reports, 8(1). https://doi.org/10.1038/s41598-018-23976-1

[60] Ryali, S., Zhang, Y., De Los Angeles, C., Supekar, K., & Menon, V. (2024). Deep learning models reveal replicable, generalizable, and behaviorally relevant sex differences in human functional brain organization. Proceedings of the National Academy of Sciences, 121(9). https://doi.org/10.1073/pnas.2310012121

[61] Chen, A. A., Srinivasan, D., Pomponio, R., Fan, Y., Nasrallah, I. M., Resnick, S. M., Beason-Held, L. L., Davatzikos, C., Satterthwaite, T. D., Bassett, D. S., Shinohara, R. T., & Shou, H. (2022). Harmonizing functional connectivity reduces scanner effects in community detection. NeuroImage, 256, 119198. https://doi.org/10.1016/j.neuroimage.2022.119198

[62] Mueller, S., Wang, D., Fox, M. D., Pan, R., Lu, J., Li, K., Sun, W., Buckner, R. L., & Liu, H. (2015). Reliability correction for functional connectivity: Theory and implementation. Human Brain Mapping, 36(11), 4664–4680. https://doi.org/10.1002/hbm.22947

[63] Henschel, L., Conjeti, S., Estrada, S., Diers, K., Fischl, B., & Reuter, M. (2020). FastSurfer - A fast and accurate deep learning based neuroimaging pipeline. NeuroImage, 219, 117012. https://doi.org/10.1016/j.neuroimage.2020.117012

[64] Hoffmann, M., Hoopes, A., Greve, D. N., Fischl, B., & Dalca, A. V. (2024). Anatomy-aware and acquisition-agnostic joint registration with SynthMorph. Imaging Neuroscience, 2, 1–33. https://doi.org/10.1162/imag_a_00197

[65] Ren, J., An, N., Lin, C., Zhang, Y., Sun, Z., Zhang, W., Li, S., Guo, N., Cui, W., Hu, Q., Wang, W., Wu, X., Wang, Y., Jiang, T., Satterthwaite, T. D., Wang, D., & Liu, H. (2024). DeepPrep: An accelerated, scalable, and robust pipeline for neuroimaging preprocessing empowered by deep learning. bioRxiv (Cold Spring Harbor Laboratory). https://doi.org/10.1101/2024.03.06.581108

99